General Local-Equilibrium Chromatographic Theory for Eluents Containing Adsorbing Buffers

Douglas D. Frey, Chittoor R. Narahari, and Christy D. Butler
Dept. of Chemical and Biochemical Engineering, University of Maryland Baltimore County, Baltimore, MD 21250

An efficient, general strategy was developed for numerically solving the system of equations that describe a pH gradient under local-equilibrium conditions when the elution buffer contains arbitrary numbers of both adsorbed and unadsorbed buffering species (weak electrolytes) and for a weak- or strong-base ion-exchange column packing. Since the method involves the solution of algebraic equations, instead of partial differential equations, it can be used to rapidly determine the effluent pH profile given the adsorption equilibrium constants for the buffering species. It can also be used iteratively to determine the adsorption equilibrium constants for the buffering species from an experimentally determined effluent pH profile as well as to determine the composition of the elution buffer required to achieve a desired shape for the pH gradient given the adsorption equilibrium constants for the buffering species. The calculation method is verified experimentally and used to illustrate the behavior of chromatographic methods which employ retained pH and ionic strength gradients.

Introduction

A number of chromatographic methods for proteins utilize retained pH gradients, that is, pH gradients which travel through the column more slowly than the velocity of an unadsorbed solute. These methods include the analytical-scale technique of chromatofocusing, which employs a synthetic polymer buffer containing large numbers of individual buffering species (weak electrolytes) to produce a linear pH gradient (Sluyterman and Elgersma, 1978; Sluyterman and Wijdeness, 1978; Amersham Pharmacia Biotech, 1980), the preparative-scale technique of buffer-focusing chromatography, which typically employs mixtures of well-defined buffering species to produce a gradient consisting of multiple stepwise pH fronts (Frey et al., 1995; Frey, 1996; Hearn and Lyttle, 1981; Hutchens et al., 1986a,b), as well as certain variations of displacement chromatography where a retained pH front formed using adsorbed buffering species is utilized as a protein displacer (Narahari et al., 1998). As discussed by Frey et al. (1995) and Frey (1996), retained gradients suitable for these applications can be formed whether or not the column packing has a buffering capacity provided that the buffering species present are adsorbed by the packing and have properly chosen concentrations.

The detailed behavior of chromatographic processes employing retained pH gradients can be investigated using numerical calculations which account for both equilibrium and mass-transfer behavior, and which involve the solution of coupled systems of partial differential equations (Frey et al., 1995). However, this approach tends to be unsuitable for routine design and optimization purposes, especially when significant numbers of buffering species are present, since it generally requires large computer resources. One alternative is to neglect mass-transfer resistances and assume that the liquid and adsorbed phases are in equilibrium throughout the column. Local-equilibrium theories of this type are well suited for the case of large numbers of buffering species since they yield relatively simple systems of coupled algebraic equations. In addition, despite their use of simplifying assumptions, local-equilibrium theories still yield the essential features of the pH gradient needed for the basic design and optimization of chromatographic processes, such as the transit times for the pH fronts and the compositions of intermediate plateaus on the pH profile.

Analytical solutions to local-equilibrium theories for certain presaturation and elution conditions where adsorbed

Correspondence concerning this article should be addressed to D. D. Frey.
Current address of C. R. Narahari: Immunex Corporation, Seattle, WA 98101.
Current address of C. D. Butler: Dept. of Biomedical Engineering, Case Western Reserve University, Cleveland, OH 44106.

buffering species are present are discussed by Helfferich and Bennett (1984a,b) and Frey (1996). In the present study these approaches are extended, and an efficient, general strategy is developed which can accommodate arbitrary numbers and types of buffering species. The method developed here is suitable, therefore, for investigating chromatographic processes which employ moderate to large numbers of weak-acid and weak-base buffering species with defined physical properties, as well as for synthetic polymer buffer systems in which case a large number of buffering species can be used to approximate the pH titration curve of actual elution buffer.

Acid-Base Equilibrium Relations

For monofunctional weak-acid or weak-base buffering species having only monovalent ionic forms, the acid-base dissociation reactions can be written

$$A_i^o \rightleftharpoons A_i^- + H^+ \tag{1}$$

$$B_i^+ \rightleftharpoons B_i^o + H^+ \tag{2}$$

where A_i^- and A_i^o are the negatively charged and neutral forms of the acidic (anion-forming) buffering species A_i, and B_i^+ and B_i^o are the positively charged and neutral forms of the basic (cation-forming) buffering species B_i. In this article the symbols A and B denote either a buffering species (such as A_i) or any of the charged forms of the buffering species (such as A_i^-) according to context. Equations 1 and 2 lead to the following equilibrium relations

$$K_{A_i} = C_{A_i^-} C_{H^+} / C_{A_i^o} \tag{3}$$

$$K_{B_i} = C_{B_i^o} C_{H^+} / C_{B_i^+} \tag{4}$$

Equation 3 yields the following expressions for the amount of each form of A_i present in terms of the total amount present, with similar expressions also applying to B_i

$$C_{A_i^o} = \frac{C_{H^+} C_{A_i}}{C_{H^+} + K_{A_i}} \tag{5}$$

$$C_{A_i^-} = \frac{K_{A_i} C_{A_i}}{C_{H^+} + K_{A_i}} \tag{6}$$

If inert ions (ions such as Na^+ or Cl^- which do not participate in acid-base equilibrium, denoted here as I^+ and I^-) are present, the liquid-phase electroneutrality condition can be written as

$$C_{I^+} - C_{I^-} - \sum_{i=1}^{N_A} \frac{K_{A_i} C_{A_i}}{K_{A_i} + C_{H^+}} + \sum_{i=1}^{N_B} \frac{C_{H^+} C_{B_i}}{K_{B_i} + C_{H^+}} + C_{H^+} - \frac{K_w}{C_{H^+}} = 0 \tag{7}$$

where K_w is the dissociation constant for water. When the total amounts of each buffering species are specified, the solution of Eq. 7 yields C_{H^+}, which can be substituted into Eqs. 5 and 6 and the corresponding equations for B_i to determine the concentrations of all ions present.

Adsorption Equilibrium for Buffering Species

For simplicity, the following development applies to the case of an anion-exchange adsorbent where the adsorption of cations formed from the buffering species is ignored. Since at equilibrium the chemical potential of any electrically neutral combination of ions is the same in the adsorbed and liquid phases, an expression that accounts for the adsorption of the anionic species A_i^- can be written

$$(q_{H^+})^{-z_{A_i^-}} q_{A_i^-} = K_{A_i^- ads} (C_{H^+})^{-z_{A_i^-}} C_{A_i^-} \tag{8}$$

where for convenience H^+ is used to form the electrically neutral ion combination despite the fact that it is assumed subsequently that the concentration of this ion is small enough to be neglected in the electroneutrality condition. In Eq. 8, $q_{A_i^-}$ denotes the equilibrium quantity of A_i^- in the adsorbed phase per unit volume of particle, not including the buffering species in the particle pores, and $K_{A_i^- \text{ads}}$ is an equilibrium parameter which accounts for osmotic pressure effects and thermodynamic nonidealities. This latter parameter is assumed to be independent of composition. For the case of a weak-base ion-exchanger, the ionizable functional groups attached to the adsorbent (denoted as q_{R_i}) are included in the adsorbent electroneutrality condition which, assuming there are no cations other than H^+ adsorbed, can be written as

$$\sum_{i=1}^{N_A} q_{A_i} - \sum_{i=1}^{N_R} \frac{q_{H^+} q_{R_i}}{K_{R_i} + q_{H^+}} + q_{H^+} - \frac{K_{w,ads}}{q_{H^+}} = 0 \tag{9}$$

For the case of a strong-base ion exchanger, and if the concentrations of H+ and OH- are assumed to be small compared to the other ions present, then the electroneutrality condition for the adsorbed phase can be written

$$q_R = \sum_{i=1}^{N_A} q_{A_i^-} \tag{10}$$

where q_R is the total ion-exchange capacity. Equations 8 and 10 can be combined to yield an explicit expression for the total amount of adsorbed buffering species

$$q_{A_i^-} = \frac{q_R K_{A_i} C_{A_i} / (C_{H^+} + K_{A_i})}{\sum_{j=1}^{N_A} K_{A_j^- A_i^-, ads} K_{A_j} C_{A_j} / (C_{H^+} + K_{A_j})} \tag{11}$$

In Eq. 11, $K_{A_j^- A_i^-, \text{ads}}$ is the ion-exchange equilibrium selectivity, which is given by the ratio $K_{A_j^-, \text{ads}} / K_{A_i^-, \text{ads}}$. With the assumption that only anions are adsorbed ($q_{A_i} = q_{A_i^-}$), the ion-exchange selectivities $K_{A_j^- A_i^-, ads}$ determine the adsorbed-phase composition, and one of the parameters $K_{A_i^-, ads}$ can be set arbitrarily to unity. Equation 11 is similar to an equation developed by Jones and Carta (1993) except that in Eq. 11 the ion-exchange selectivity is assumed constant and the concentrations of H^+ and OH^- are assumed to be small enough to be ignored in the electroneutrality relations. These two assumptions also apply to all the calculations in the remainder of this study.

To account for the adsorption of neutral forms of the buffering species, it will be assumed that the equilibrium amount of the neutral form adsorbed is linearly related to the amount of this form in the liquid phase, in which case the total amount of adsorbed buffering species (q_{A_i}) is given by adding the product $C_{A_i^o} K_{A_i^o ads}$ to $q_{A_i^-}$, where $q_{A_i^-}$ is calculated as described above and $K_{A_i^o ads}$ is an adsorption equilibrium constant (Reichenberg and Wall, 1956; Feitelson, 1969). The selection of a linear adsorption equilibrium relation reflects the fact that in this study the liquid-phase concentrations of the buffering species are small compared to the ion-exchange capacities of the column packings used so that the adsorption of neutral species is generally a minor contributor to the total amount adsorbed.

Additional details concerning the description of adsorption equilibrium used in this study are given by Frey et al. (1995) and Strong and Frey (1997). Related approaches are discussed by Klein et al. (1982), Jones and Carta (1993), Jansen et al. (1996), and Bellot et al. (1999). Another related approach in which adsorption is represented entirely as the complexation of neutral forms of buffering species by neutral forms of the functional groups on the column packing is given by Garcia and King (1989) and Yoshida et al. (1995). The equivalence of this latter approach and the approach used in this study in terms of the adsorption isotherms which apply is discussed by Frey (1997).

Coherence Conditions

The differential material-balance relation for any buffering species can be written

$$\alpha \frac{\partial C_{A_i}}{\partial t} + \alpha v_{fluid} \frac{\partial C_{A_i}}{\partial x} + (1-\alpha) \frac{\partial \left(\epsilon C_{A_i} + q_{A_i} \right)}{\partial t} = 0 \quad (12)$$

For uniform presaturation and elution conditions, the velocity of a stepwise change in composition (a self-sharpening front) consistent with Eq. 12 is given by (Wankat, 1990)

$$v_{\Delta C} = \frac{v_{fluid}}{1 + \dfrac{(1-\alpha)\epsilon}{\alpha} + \dfrac{(1-\alpha)}{\alpha} \left[\dfrac{q_{A_i,u} - q_{A_i,d}}{C_{A_i,u} - C_{A_i,d}} \right]} \quad (13)$$

where the subscripts u and d denote the upstream and downstream composition plateaus.

In this study, it is assumed that all composition changes are coherent in the sense that a stepwise composition change continues to span a fixed composition range for every component as it travels downstream (Helfferich and Klein, 1970). Under these conditions, Eq. 13 implies that the following relation applies to any two buffering species (that is, species A_i and A_j)

$$\frac{q_{A_i,u} - q_{A_i,d}}{C_{A_i,u} - C_{A_i,d}} = \frac{q_{A_j,u} - q_{A_j,d}}{C_{A_j,u} - C_{A_j,d}} \quad (14)$$

Note that, for a retained front (that is, a front with a velocity less than that of an unadsorbed solute), the concentrations of all unadsorbed buffering species and unadsorbed inert ions do not vary across the front, in which case those components have the same concentrations throughout the column as in the elution buffer.

Solution Strategy and Numerical Methods

Although the algebraic equations in the preceding section can be solved for arbitrary presaturation and elution buffer compositions, the cases discussed below tend to be the most useful in preparative or analytical chromatography and, in particular, are those where the pH decreases monotonically over the major portion of the gradient.

Strong-base ion-exchange adsorbent presaturated with a weak-acid buffering species (Case 1)

This case is discussed by Frey et al. (1995), Frey (1996), and Narahari et al. (1998). As illustrated by the numerical calculations shown in Figure 1a, if an anion-exchange column

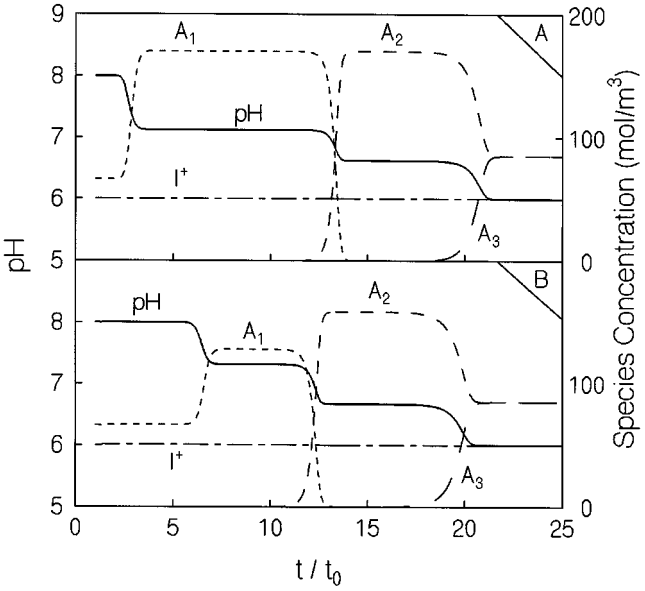

Figure 1. Calculated effluent pH and buffering species concentration profiles for Cases 1 and 2.

Case 1 (part A) involves a strong-base anion-exchange column packing where $\alpha = 0.35$, $\epsilon = 0$, $\nu_{\text{fluid}} = 0.1$ cm/s, $L = 10$ cm, $d_p = 90$ μm, and $q_R = 1$ M. The symbol I^+ denotes an inert cation while A_1, A_2, and A_3 denote weak-acid buffering species with pK_a values of 7.5, 7, and 6, respectively. The column was presaturated at pH 8 with 50 mol/m^3 I^+ and 66 mol/m^3 A_1 and eluted with 50 mol/m^3 I^+ and 83 mol/m^3 of both A_2 and A_3. $K_{A_i^-,\text{ads}} = 1$ and $K_{A^0,\text{ads}} = 1$ for all buffering species and $t_0 = L/\nu_{\text{fluid}}$. (b) Case 2 (part B) involves a weak-base anion-exchange column packing where $\alpha = 0.35$, $\epsilon = 0$, $\nu_{\text{fluid}} = 0.1$ cm/s and where there is one strong-base and one weak-base functional group on the column packing both with concentrations of 500 mol/m^3 and with the latter having a pK_a of 8.25. The symbol I^+ denotes an inert cation while A_1, A_2, and A_3 denote weak-acid buffering species with pK_a values of 7.5, 7, and 6, respectively. The column was presaturated at pH 8 with 50 mol/m^3 I^+ and 66 mol/m^3 A_1 and eluted with 50 mol/m^3 I^+ and 83 mol/m^3 of both A_2 and A_3. $K_{A_i^-,\text{ads}} = 1$, $K^0_{Ai,ads} = 1$, and $D_{\text{eff}} = 8 \times 10^{-11}$ m^2/s for all buffering species and $t_0 = L/\nu_{\text{fluid}}$.

is presaturated with a weak-acid buffering species titrated with a strong base (such as, NaOH) to the presaturation pH and eluted with a mixture of weak-acid buffering species titrated with a strong base to the elution pH, and also if the buffering species present in the presaturation buffer has the lowest adsorption affinity (the lowest value of q_{A_i}/C_{A_i}) of all the buffering species present, then the effluent concentration profile consists of one unretained front where the concentration of the presaturation buffering species changes, and a series of retained fronts which are generally self-sharpening.

Figure 1a also indicates that the buffering species appear in the effluent one-by-one in order of their adsorption affinities. This behavior follows directly from Eq. 13 and the observation that a species appearing in the effluent profile is present on only the upstream side of a front so that the quantity in square brackets in Eq. 13 reduces to $q_{A_i,u}/C_{A_i,u}$, that is, the adsorption affinity on the upstream side of the front where the buffering species appears. Note that for the case where there is no adsorption of neutral species, the relative adsorption affinity of a pair of buffering species is given by combining Eqs. 6 and 10 to yield

$$\frac{q_{A_j^-} C_{A_i}}{q_{A_i^-} C_{A_j}} \equiv K_{A_j^- A_i^-,ads} \left(\frac{K_{A_j}}{K_{A_i}} \frac{10^{-pH} + K_{A_i}}{10^{-pH} + K_{A_j}} \right) \tag{15}$$

The development given above implies that if there are n buffering species in the elution buffer, then there are a total of $n+1$ pH fronts in the effluent profile and that, with the exception of the presaturation plateau, the sum of the buffering species concentrations present on any plateau is equal to the sum of those concentrations in the elution buffer provided that there is no adsorption of the neutral forms of the buffering species.

If Eq. 11 is written for the two buffering species A_i and A_j and substituted into Eq. 14, the result is the coherence condition written entirely in terms of the liquid-phase pH and liquid-phase concentrations of the buffering species. Consider the situation where the pH and composition of the n acidic buffering species in the elution buffer are specified along with the pH and composition of the presaturation buffer. Since the acidic buffering species with the highest adsorption affinity will be absent from the plateau adjacent to the elution plateau (that is, the plateau on the downstream side of the slowest pH front), the pH and concentrations of the $n-1$ acidic buffering species on this plateau can be solved for using the liquid-phase electroneutrality condition (Eq. 7) along with $n-1$ independent versions of the coherence condition obtained using $n-1$ pairs of buffering species present in the elution buffer. After obtaining the composition and pH in this manner on the plateau adjacent to the elution plateau, this process can be repeated to solve for the pH and concentrations of the $n-2$ buffering species present on the next plateau in the downstream direction.

For the particular case where there is no adsorption of the neutral forms of the buffering species and when the composition of the presaturation buffer is specified, then the concentration of the single buffering species on the next two plateaus in the upstream direction from the presaturation plateau is equal to the sum of concentrations of the buffering species in the elution buffer, and the concentrations and pH values associated with these plateaus will not be considered unknown variables. In addition, the requirement that the sum of the concentrations of the buffering species on any particular plateau (with the exception of the presaturation plateau) equals the sum of those concentrations in the elution buffer can replace any one of the coherence conditions on each plateau in the system of equations to be solved. In this case, when there are n buffering species in the elution buffer, there are $n-2$ independent subsystems of algebraic equations containing a total of $(n-2)(n+3)/2$ independent equations and an equal number of unknowns. The unknowns are the liquid-phase compositions and pH values on all the intermediate plateaus, with the exceptions noted above. The equation subsets can be solved sequentially starting at the elution plateau, and consist of the coherence conditions for a particular pH front together with the liquid-phase electroneutrality condition for the plateau on the upstream side of that front.

Weak-base ion-exchange adsorbent presaturated with a weak-acid buffering species (Case 2)

This case is discussed by Frey et al. (1995) and Frey (1996) and illustrated by the numerical calculations in Figure 1b. As shown in the figure, when a weak-base anion-exchange column is presaturated with a single weak-acid buffering species, and then eluted with a mixture of weak-acid buffering species all of which have adsorption affinities larger than that of the presaturation buffering species, then the general behavior is similar to Case 1, except that the first front to exit the column (the front adjacent to the presaturation plateau) is retained by the column. In addition, the sum of the concentrations of the buffering species on each composition plateau is no longer equal to that sum in the elution buffer even when there is no adsorption of the neutral forms of the buffering species. Nevertheless, as was the situation in Case 1, when there are n buffering species in the elution buffer, there are a total of $n+1$ pH fronts in effluent profile.

If Eqs. 6, 8, and 14 are combined, the coherence condition can be written in terms of the liquid-phase buffering species concentrations and the pH in the liquid and adsorbed phases as

$$\frac{K_{A_i^- A_j^-,ads}(C_{H^+,u}/q_{H^+,u})^{z_{A_i^-}} \left(C_{H^+,u} + K_{A_i}\right) C_{A_i,u}/K_{A_i} - K_{A_i^- A_j^-,ads}(C_{H^+,u}/q_{H^+,u})^{z_{A_i^-}} \left(C_{H^+,d} + K_{A_i}\right) C_{A_i,d}/K_{A_i}}{C_{A_i,u} - C_{A_i,d}}$$

$$= \frac{(C_{H^+,u}/q_{H^+,u})^{z_{A_j^-}} \left(C_{H^+,u} + K_{A_j}\right) C_{A_j,u}/K_{A_j} - (C_{H^+,u}/q_{H^+,u})^{z_{A_j^-}} \left(C_{H^+,d} + K_{A_j}\right) C_{A_j,d}/K_{A_j}}{C_{A_j,u} - C_{A_j,d}} \tag{18}$$

Furthermore, if the pH and composition of the elution buffer is specified, then the liquid-phase pH and composition of all other composition plateaus can be determined using methods similar to those described for Case 1 by considering each remaining plateau in sequence starting with the plateau adjacent to the elution plateau. For example, if the elution buffer contains n acidic buffering species, then the liquid- and adsorbed-phase pH and the liquid-phase concentrations of the $n-1$ acidic buffering species present on the composition plateau adjacent to the elution plateau can be determined by solving $n-1$ independent versions of Eq. 18, written for $n-1$ pairs of acidic buffering species present in the elution buffer, and the electroneutrality conditions for the liquid and adsorbed phases (Eqs. 9 and 11). Therefore, when n acidic buffering species are present in the elution buffer, there are n independent subsets of equations containing a total of $(n^2+3n+2)/2$ equations and an equal number of unknown variables to solve. The unknown variables consist of the concentrations of the buffering species and the liquid- and adsorbed-phase pH values on a particular plateau, while the equation subsets consist of the coherence conditions for a particular front and the electroneutrality conditions for the liquid and adsorbed phases for the plateau on the downstream side of that front.

Weak-base ion-exchange adsorbent presaturated with a weak-base buffering species (Case 3)

This case is also discussed by Frey et al. (1995) and Frey (1996) and corresponds to conditions typically recommended for use with commercially available chromatofocusing adsorbents and buffers (Amersham Pharmacia Biotech, 1980). As shown by the numerical calculations shown in Figure 2, when a column is presaturated with a weak-base buffering species titrated to the presaturation pH with a strong acid, and eluted with an elution buffer containing several weak-acid buffering species titrated to the elution pH with a strong base, all the pH fronts formed are retained by the column. As in Cases 1 and 2, the buffering species present in the elution buffer appear one-by-one in order of their adsorption affinities in a series of retained fronts.

As also shown in Figure 2, the inert anion present in the presaturation buffer (the anion associated with the strong acid used to form the presaturation buffer) tends to increase somewhat in the first front to exit the column, to be nearly constant for several subsequent fronts, and to then decrease to zero in one or more final fronts that are nonself-sharpening in nature. Note that for a nonself-sharpening front, only the velocity of the front's center and not the entire front shape can be determined by the methods described here. In addition, the pH may increase in the upstream direction on the last front to exit the column, instead of decreasing in that direction as is the case for all the other fronts considered here, so that a pH minimum may occur in the gradient. Nevertheless, as was the situation in Cases 1 and 2, when there are a total of n buffering species in the elution buffer, there are $n+1$ pH fronts in the effluent profile. Finally, note that, for all three cases discussed here, a determination of whether a particular front is self-sharpening or nonself-sharpening can be performed using, among a variety of alternatives, the entropy admissibility criterion discussed by Frey (1990).

In general for Case 3, the coherence conditions for all the fronts must be solved simultaneously together with the electroneutrality conditions in the liquid and adsorbed phases for each plateau in order to determine the compositions on each plateau. However, as shown in Figure 2, it may be a reasonable approximation under some conditions to assume that the concentration of the inert anion is constant across all the fronts, except the final one to exit the column. Using this assumption, the structure of the equations to be solved becomes similar to Case 2, that is, the unknowns for each plateau are the buffering species concentrations and the pH values of the liquid and adsorbed phases. These variables can be solved for using the liquid- and adsorbed-phase electroneutrality conditions and one coherence conditions for each component on the plateau. Therefore, if there are a total of n buffering species in the elution buffer, there will be n subsystems of equations, which in this case contain a total of $n(n+5)/2$ equations and an equal number of unknown variables to solve for. In addition, the equation subsystems can be solved sequentially starting at the upstream end of the column as in Case 2.

Experimental Methods

Chromatography was performed using either Q Sepharose Fast Flow strong-base ion-exchange stationary phase or PBE 94 weak-base ion-exchange stationary phase (Amersham Pharmacia Biotech, Piscataway, NJ) packed into either a 10 cm $\times$ 1 cm I.D. or a 20 cm $\times$ 1 cm I.D. glass column (Omnifit, Cambridge, U.K.), or using a 5 cm $\times$ 0.5 cm I.D. packed glass column containing Mono Q strong-base ion-exchange stationary phase, also obtained from Amersham Pharmacia Biotech. The chromatography equipment consisted of a SpectraSystem P4000 gradient pump, a SpectraSystem UV 2000 absorbance detector, and a SpectraSystem SCM 1000 Vacuum Membrane Degasser (Thermo Separation Products, San Jose, CA). The pH was measured by a Sensorex pH electrode seated into a flow cell and connected to an Orion Model 701A Ionalyzer pH meter. The buffering species were 3-(N-morpholino)propanesulfonic acid (MOPS), 2-(N-morpholino)ethanesulfonic acid (MES), N-Tris(hydroxymethyl)methylglycine (Tricine), 2-amino-2-hydroxymethyl-1,3-propanediol (Tris), acetic acid, and formic acid (Sigma, St. Louis, MO). All buffers were vacuum filtered before use.

Determination of Adsorption Equilibrium Constants

Several experiments in which a given packing material was presaturated with one buffering species and eluted with second buffering species were performed to determine the adsorption equilibrium constants for the two species. To facilitate the interpretation of the data, the column was presaturated with the buffering species having the highest adsorption affinity of the pair being investigated so that the concentration fronts formed were primarily nonself-sharpening in nature and therefore had shapes that were more sensitive to the values of adsorption equilibrium constants as compared to the case where self-sharpening fronts exist. Values for the equilibrium constants were determined by manually compar-

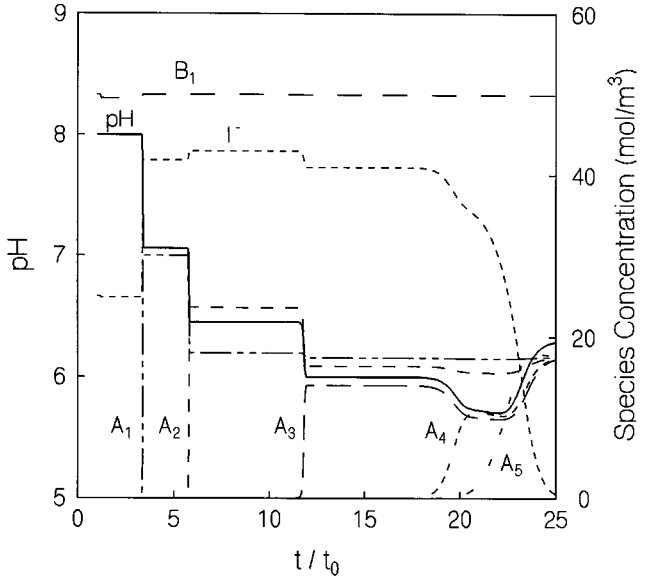

Figure 2. Effluent pH and buffering species concentration profiles for Case 3.

Calculations are for a weak-base anion-exchange column packing where $\alpha = 0.35$, $\epsilon = 0$, $\nu_{\text{fluid}} = 0.06$ cm/s, $L = 10$ cm, $d_p = 45$ μm. It was assumed there were 15 types of functional groups on the column packing, with 14 of the groups each having concentrations of 26 mol/m^3 and pK_a values evenly spanning the range from 3 to 9.5 and with the final functional group being strongly basic and having a concentration of 430 mol/m^3. The symbol I^- denotes an inert anion, B_1 denotes a weak-base buffering species with a pK_a value of 8.0, and A_1, A_2, A_3, A_4, and A_5 denote weak-acid buffering species with pK_a values of 8, 7, 6, 5, and 4, respectively. The column was presaturated at pH 8 with 50 mol/m^3 B_1 and 25 mol/m^3 I^- and eluted with 50 mol/m^3 B_1 and 17.5 mol/m^3 of all the acidic buffering species. $K_{A_i^-,\text{ads}} = 1$, $K^0_{A_i,\text{ads}} = 1$, and $D_{\text{eff}} = 8 \times 10^{-7}$ cm^2/s for all buffering species and $t_0 = L/\nu_{\text{fluid}}$.

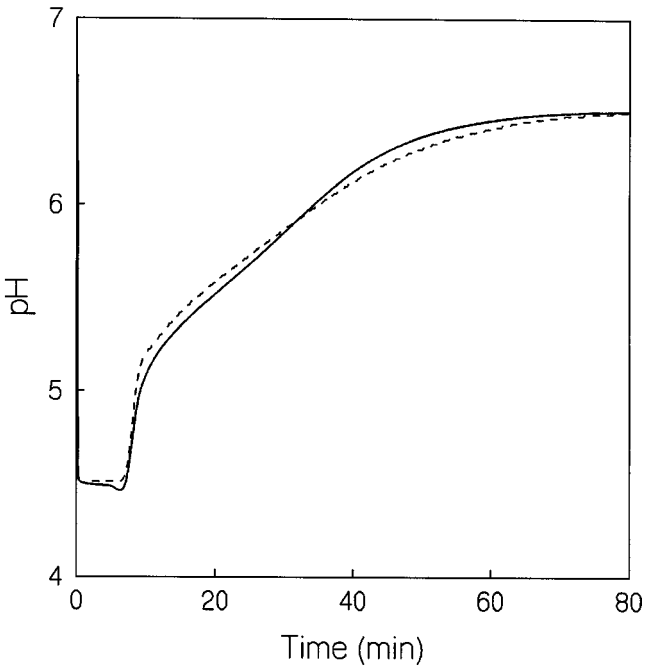

Figure 3. Comparison between experimentally measured (solid line) and theoretically calculated (dashed line) effluent pH profiles.

Conditions correspond to a 8.5×1 cm I.D. column packed with Q Sepharose Fast Flow presaturated with 25 mol/m^3 NaOH titrated with acetic acid to pH 4.5 and eluted with 25 mol/m^3 NaOH titrated with MES to pH 6.5. The flow rate was 1 mL/min. The parameters used in the theoretical calculations are described in Table 1.

ing measured effluent pH profiles with profiles calculated using the numerical method described by Frey et al. (1995). Although the numerical method used accounts for mass-transfer resistances, these effects are small for the case where the fronts are primarily nonself-sharpening so that the fitted equilibrium parameters are insensitive to the assumed mass-transfer parameters.

Figure 3 gives typical results of the procedure just described for the Q Sepharose Fast Flow column packing. In general, the pH profiles in these experiments consist of an initial relatively steep front followed by a small plateau, which is followed in turn by a broader front. However, when the pH change for the two fronts is in the same direction, such as in Figure 3, and when the pH plateau between the two fronts is very small, then the entire profile appears to be a single front. The types of pH profiles shown in Figure 3 are especially convenient for fitting experiments to theory since the position of the early part of the profile (the first front, which does not involve the ion exchange of adsorbed ions) is determined by the adsorption equilibrium constants of the neutral forms of the buffering species while the shape of the latter part of the profile (the second front, where one ion in the adsorbed phase is exchanged for another ion) is determined primarily by the adsorption equilibrium constants for the charged forms of the buffering species.

Tables 1 and 2 summarize results from the data fitting procedure for the Q Sepharose Fast Flow and PBE 94 column packings. For simplicity in fitting the data, and because of the dilute conditions used, the pore volume of the particles was neglected, that is, it was assumed that $\epsilon = 0$ so that the amounts adsorbed are based in effect on the total amount of buffering species within the exterior surface of the adsorbent particles, including the buffering species in the particle pores.

The results shown in Tables 1 and 2 indicate that, for the two column packings, the adsorption capacity varied somewhat depending on what pair of buffering species was employed. Nevertheless, the values for the total adsorption and buffering capacities shown in Tables 1 and 2 agree reasonably well with those reported by the column packing manufacturer (Amersham Pharmacia Biotech, 1980). The results shown also indicate that within the experimental error, a single value for $K_{A_i^0,ads}$ of 1.25 adequately describes the adsorption of the neutral forms of the buffering species. Furthermore, this value for $K_{A_i^0,ads}$ is comparable to the value for this parameter determined by other investigators for similar systems (Reichenberg and Wall, 1956). In general, the values for $K_{A_i^-,ads}$ and $K_{A_i^0,ads}$ given in Tables 1 and 2 are accurate to within approximately 25% and 50%, respectively, as determined by the sensitivity of the calculated pH profiles in Figure 3 to the values of those parameters. Although the fact that the effluent pH profile tends to be insensitive to the adsorption equilibrium constant means that some uncertainty

Table 1. Adsorption Equilibrium Constants and other Properties for Various Buffering Species on Q Sepharose Fast Flow*

	pK_a	MW	$K_{A_i^-,ads}$	q_R
Acetate	4.8	60	1.0	-
MES	6.1	195.2	0.70	270
MOPS	7.2	209.3	0.94	220
Tricine	8.1	179.2	1.2	210

*Values correspond to experiments where either Tricine, MES, or MOPS was used to elute a column initially presaturated with the acetate ion. $\alpha = 0.35$ and $\epsilon = 0$ were assumed in the determination of the values shown and, for all the species, the approximate best fitting value for $K_{A_i^0,ads}$ was 1.25. Representative experimental conditions are described in the caption to Figure 3.

results when these constants are determined from the profile, it also means that highly accurate adsorption equilibrium constants are generally not needed to predict the effect of the elution buffer composition on the effluent pH profile, as demonstrated below.

Related studies of ion-exchange equilibrium for aliphatic carboxylic acids performed by other workers indicate that $K_{A_i^-,ads}$ tends to decrease with increasing molecular weight (with decreasing pK_a) although carboxylic acids that are relatively hydrophobic can have larger values of $K_{A_i^-,ads}$ than might be expected on the basis of their size alone (Diamond and Whitney, 1966). An example of this trend is given by the behavior of the strong-base styrene-divinylbenzene anion exchanger Dowex-1 X10 manufactured by Dow for which the ion-exchange selectivities ($K_{A_j^-A_i^-,ads}$) for formate and chloride ions, for acetate and chloride ions, and for butyrate and chloride ions, are 0.21, 0.13, and 0.26, respectively (Diamond and Whitney, 1966). In a previous study in this laboratory, the method illustrated in Figure 3 was used to determine that the ion-exchange selectivity for formate and acetate ions on Q Sepharose Fast Flow is 1.6, which is in agreement with the molecular weight trend just mentioned and the ratio $K_{\text{formate}^-\text{Cl}^-,ads}/K_{\text{acetate}^-\text{Cl}^-,ads}$ using the selectivities reported above (Strong and Frey, 1997). The apparent lack of a definitive trend with molecular weight or pK_a in Tables 1 and 2 is therefore likely due to the complex effects of the size, pK_a, and hydrophobicity of the buffering species on their adsorption affinity.

Table 2. Adsorption Equilibrium Constants and Other Properties for Various Buffering Species on PBE 94*

	$K_{A_i^-,ads}$	$q_{R_{15}}$
Acetate	1.0	–
MES	0.85	240
MOPS	0.85	210
Tricine	0.76	200

*The functional groups on the column packing were accounted for using 14 types of weak-base groups with concentration of 35 mol/m^3 and pK_a values that span the range from 3 to 9.5 in 0.5 unit increments with an additional strong-base functional group, denoted as $q_{R_{15}}$, having a concentration given in the table. Values correspond to experiments where either Tricine, MES, or MOPS was used to elute a column initially presaturated with the acetate ion. $\alpha = 0.35$ and $\epsilon = 0$ were assumed in the determination of the values shown and, for all the species, the approximate best fitting value for $K_{A_i^0,\text{ads}}$ was 1.25. Representative experimental conditions are described in the caption to Figure 4.

Prediction of Effluent pH Profiles Using Local-Equilibrium Theory

Figure 4 illustrates a comparison of experimental data and calculations using local-equilibrium theory for Case 1 where a strong-base ion-exchange column packing is employed, where the column is originally presaturated with the buffering species having the lowest adsorption affinity, and where the column was eluted with two different mixtures of other buffering species having higher adsorption affinities. As illustrated in the figure, and as discussed previously, local-equilibrium theory yields values for the transit times of the pH fronts and the pH values on the plateaus separating these fronts which, although not a complete characterization of the effluent profile, nevertheless permits a reasonable comparison between theory and data. Note that the parameters used in the local-equilibrium calculations illustrated are taken from Table 1, except that an average value for q_R was employed. As shown, reasonably good agreement is achieved, with the small discrepancies observed likely due to the imprecision in the values of $K_{A_i^-,ads}$ and q_R used, and to the fact that $K_{A_i^-,ads}$ is likely not constant as assumed, but is instead a function of composition to some degree.

Figure 5 illustrates experimental data and calculations using local-equilibrium theory for Case 2 where a weak-base ion-exchange column packing is employed, where the column is again originally presaturated with the buffering species having the lowest adsorption affinity, and where the column is eluted with two different mixtures of other buffering species

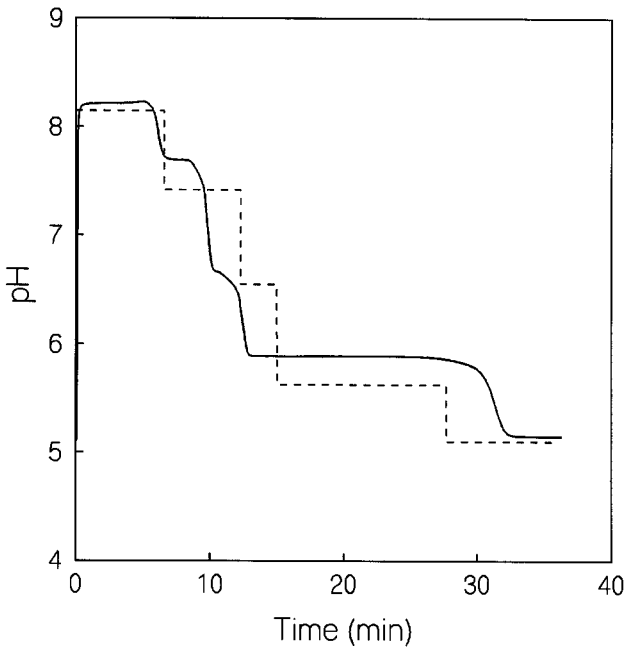

Figure 4. Comparison between experimentally measured (solid line) and theoretically calculated (dashed line) effluent pH profiles for Case 1.

Conditions correspond to a 8.5 x 1 cm I.D. column packed with Q Sepharose Fast Flow presaturated with a buffer made by titrating a 25 mol/m^3 NaOH with TRICINE to pH 8.1 and eluted with a buffer consisting of 25 mol/m^3 NaOH, 51 mol/m^3 MOPS, 61 mol/m^3 MES titrated with acetic acid to pH 5.0. The flow rate used was 1 ml/min. The parameters used in the calculations are given in Table 1.

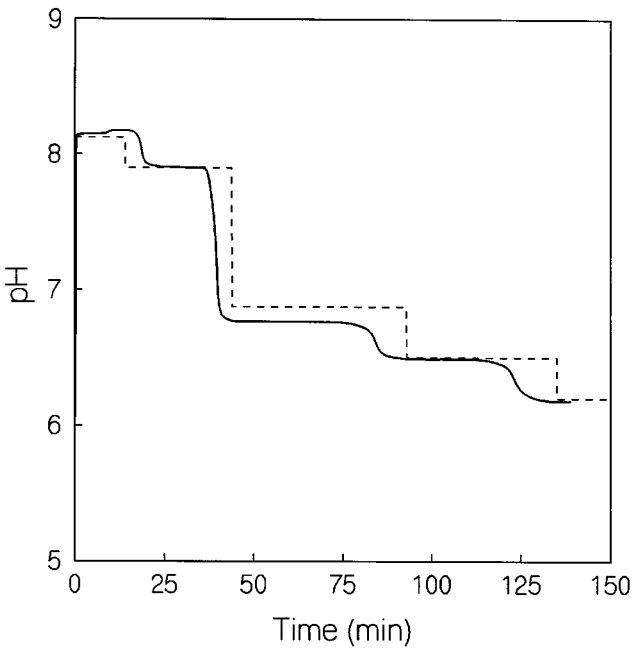

Figure 5. Comparison between experimentally measured (solid line) and theoretically calculated (dashed line) effluent pH profiles for Case 2.

Conditions correspond to a 16 x 1 cm I.D. column packed with PBE 94 presaturated with a buffer consisting of 20 mol/m^3 NaOH titrated with TRICINE to pH 8 and eluted with a buffer consisting of 20 mol/m^3 NaOH, 50 mol/m^3 MOPS and 10 mol/m^3 MES titrated with acetic acid to pH 6.0. The flow rate used was 1.0 mL/min. Parameters used for the theoretical calculations are given in Table 2.

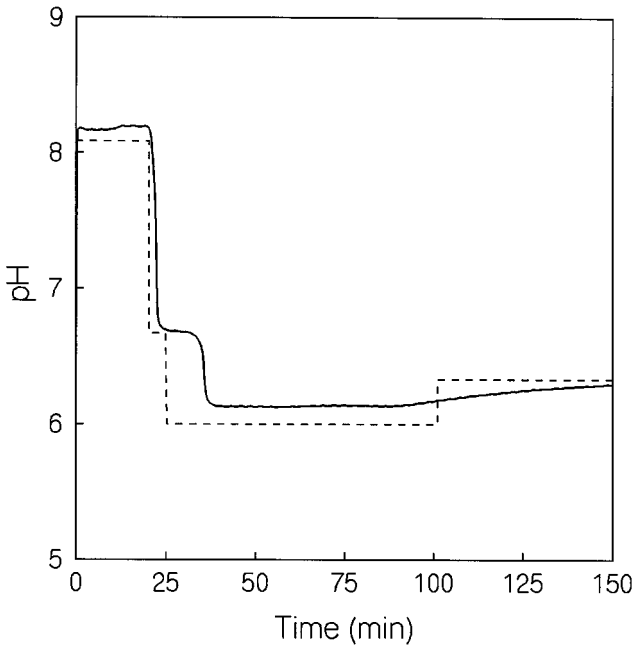

Figure 6. Comparison between experimentally measured (solid line) and theoretically calculated (dashed line) effluent pH profiles for Case 3.

Conditions correspond to a 16 x 1 cm I.D. column packed with PBE 94 presaturated with a buffer consisting of 40 mol/m^3 Tris titrated with HCl to pH 8.1 and eluted with a buffer at pH 6.2 consisting of 40 mol/m^3 Tris, 50 mol/m^3 MOPS and 50 mol/m^3 MES. The flow rate used was 1.0 mL/min. Parameters used for the theoretical calculations are given in Table 2 along with $K_{Cl^-,ads} = 2.0$.

having higher adsorption affinities. The adsorption equilibrium constants used in the calculations were again taken from Table 2, except that an average value for the concentration of the strong-base function group on the column packing ($q_{R_{15}}$) was employed. As shown, reasonably good agreement was again achieved between experiment and theory for this case.

Figure 6 illustrates a comparison between experimental data and calculations using local-equilibrium theory for Case 3 where a weak-base ion-exchange column packing was presaturated with the chloride ion, and then eluted with a mixture of MOPS and MES. The physical parameters used in the calculations were again taken from Table 2 with an average value for $q_{R_{15}}$ employed. In addition, a value of 2.0 was used for $K_{Cl^-,ads}$ in order to achieve the best agreement between theory and experiment. Note that the resulting value for the ion-exchange selectivity for the chloride and acetate ions is also 2.0, which is nearly equal to the value of 2.5 determined for this selectivity by Helfferich and Bennett (1984b) for the ion exchanger Amberlite IRA-400 manufactured by Rohm and Haas, but significantly less than the value of 7.5 determined for this selectivity for the ion exchanger Dowex-1 X10, as discussed earlier. As shown in the figure, good agreement was again achieved between theoretical results and experimental data for the conditions shown.

Simulation of a Chromatographic System Employing a Polyampholyte Elution Buffer

As discussed previously, the equations resulting from local-equilibrium theory for Case 3 can be simplified if it is assumed that the inert ion used to presaturate the column (such as the chloride ion) has a fixed concentration in the mobile phase except in the final front to exit the column where the concentration of this ion changes to its value in the elution buffer. Figure 7 illustrates a comparison of experimental data taken from the literature for the case where a commercial polyampholyte elution buffer and the PBE column packing were employed (Amersham Pharmacia Biotech, 1980) and calculations using local-equilibrium theory with the simplifications just mentioned. To perform the calculations, the polyampholyte elution buffer, which in reality consists of a very large number of individual species, was represented as a mixture of 5 weak-acid and 5 weak-base buffering species all having concentrations of 0.35 mol/m^3 so that the buffering capacity of the elution buffer was equal to that of the polyampholyte buffer used. The concentrations and properties of the functional groups attached to the PBE 94 column packing are those given in Table 2. In addition, to fit the experimental data, the values of 2.0 and 0.25 were used for the adsorption equilibrium constants for the chloride ion and for the buffering species, respectively. The latter value is less than that used for the buffering species in Tables 1 and 2, which reflects that the buffering species in the polyampholyte buffer are large hydrophilic organic ions that likely have adsorption affinities smaller than those in the tables. Other conditions are described in the caption to Figure 7. As shown in the figure, good agreement was achieved between data and

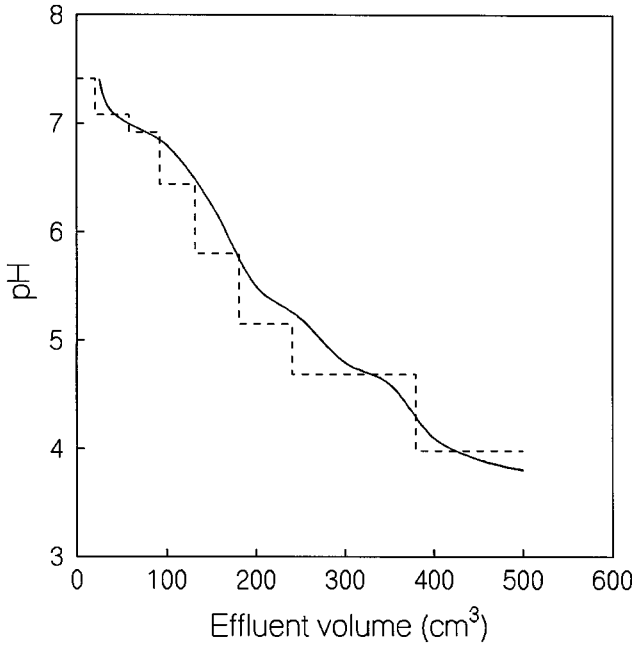

Figure 7. Comparison between experimentally measured and theoretically predicted effluent pH profiles for the case where a polyampholyte elution buffer is employed.

The polyampholyte buffer is represented as a mixture of 5 weak-acid and 5 weak-base buffering species, with pKa values of 8, 7, 6, 5 and 4 and 8, 7, 6 and 5, respectively, and with concentrations of 0.35 mol/m^3. Other parameters used in the theoretical calculations are described in Table 2. Experimental data are taken from Amersham Pharmacia Biotech (1980).

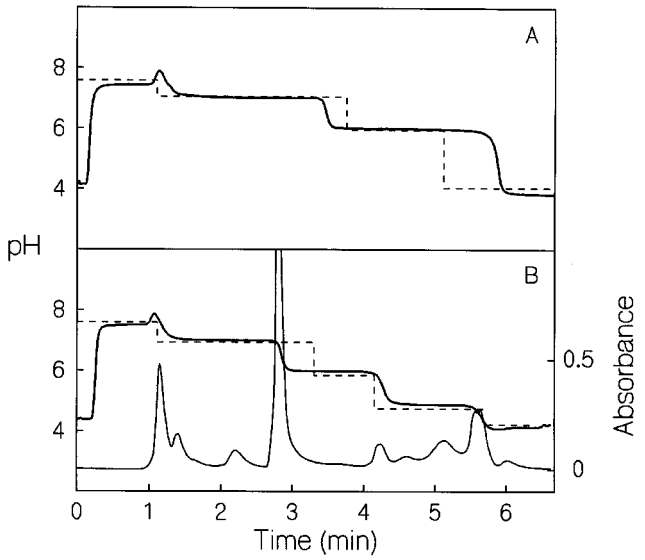

Figure 8. Comparison between experimentally measured (solid line) and theoretically calculated (dashed line) effluent pH profiles for a 5 x 0.5 cm I.D. column packed with Mono Q at a flow rate of 1 mL/min.

In part A the elution buffer was composed of 40 mol/m^3 MES and 78 mol/m^3 formic acid. In part B the elution buffer was composed of 40 mol/m^3 MES, 50 mol/m^3 acetic acid, and 53 mol/m^3 formic acid. Both experiments employed MOPS as the presaturation buffering species. The fractionation of an *E. Coli* cell lysate is also illustrated in part B which shows the UV absorbance at 280 nm in the column effluent resulting from the injection of 20 μL of lysate. Calculations correspond to $\alpha = 0.35$, $\epsilon = 0$, $q_R = 0.57$, $K_{A_i^0,ads} = 1.25$ for all the buffering species, and $K_{A_i^-,ads} = 0.60$, 0.65, 1.0, and 1.6 for MOPS, MES, acetate and formate, respectively.

theory, which indicates the calculation method has applications in the simulation of these types of systems.

Computer-Aided Design of the Elution Buffer for Protein Chromatography

In this section the numerical methods described previously are extended to permit the determination of the adsorption equilibrium constants of the buffering species from experimentally measured pH profiles consisting of multiple self-sharpening fronts, and the determination of the composition of the elution buffer needed to achieve a desired effluent pH profile from these adsorption equilibrium constants.

Figure 8 illustrates a pH gradient formed using an elution buffer containing two buffering species and a strong-base anion-exchange column packing (Strong, 1997). Also shown are local-equilibrium theory calculations in which the physical properties used were chosen to achieve the best fit to the experimental results. In particular, to fit the experimental data, distances between corresponding "corner points" (the points at the edges of the pH plateaus) for the experimental and calculated profiles were squared and summed, and the sum was then minimized by adjusting the values of the adsorption equilibrium constants and the total adsorption capacity. As illustrated, good agreement was achieved between the theoretically predicted and experimentally measured pH profiles using this procedure.

In order to demonstrate the utility of local-equilibrium theory for computer-aided design of the elution buffer composition, the numerical methods developed in this study were used to determine the concentrations of acetic and formic acids needed in the elution buffer so that this buffer has a pH of 4.2 and so that an additional pH plateau is formed in the column effluent with a pH of 4.75. To perform the design procedure, the ratio of $K_{A_i^-,ads}$ for formic and acetic acids was assumed to be 1.6, which is the value of this ratio determined for Q Sepharose Fast Flow by Strong and Frey (1997) as discussed previously, and local-equilibrium theory was employed to determine the amounts of acetic and formic acids required to achieve the desired gradient. Figure 8b illustrates a comparison of the experimentally measured and theoretically predicted pH gradient for the selected acetic and formic acid concentrations where it can be seen that the elution buffer used yields a pH gradient having the desired properties. Although the errors involved in determining the adsorption equilibrium constants by the method illustrated in Figure 8a will generally be larger than those determined using the method earlier, the effluent pH profile is largely determined by the elution buffer composition, as discussed previously, so that reasonably accurate predictions of the effluent pH profile are still possible, as shown in Figure 8b.

Figure 8b also illustrates the fractionation of proteins from an *E. coli* cell lysate achieved using the modified pH gradient described above, with the lysate used described by Narahari et al. (2001). As shown, a number of protein bands are evident in the column effluent, with the narrowest bands located on the stepwise pH fronts in the gradient due to the focusing effects present at those locations, in agreement with the discussion by Strong and Frey (1997). The results in Figure 8b, as well as similar results discussed by Strong and Frey (1997) and Narahari et al. (1998), indicate that pH gradients consisting of retained self-sharpening fronts can fractionate proteins in a manner similar to the more common technique of using multiple stepwise ionic strength gradients (Gerberding and Byers, 1998). For this reason, the numerical methods and associated computer-aided design methods illustrated in this study are likely to be of value as a means for optimizing the former type of chromatographic process.

Conclusions

An efficient, general strategy is developed for solving the system of algebraic equations describing local-equilibrium theory for retained pH gradients formed using an ion-exchange column packing and any number of adsorbed and unadsorbed buffering species in the elution buffer. The method is able to determine the position of the pH fronts and the compositions of intermediate plateaus on the effluent pH profile. Results from the method are in good agreement with experimental data and have applications in the design and optimization of chromatofocusing processes and related chromatographic methods which employ retained pH and ionic strength gradients.

Acknowledgments

Support from grant CTS 9813658 from the National Science Foundation and from NIH National Research Service Award GM 08663 from the MARC U*STAR Program at UMBC is gratefully acknowledged. We also thank Dr. John Strong at Abbott Laboratories for certain of the data in Figure 8 which were taken from Strong (1997).

Notation

C_A = concentration in liquid phase, mol/m^3
$K_{A,ads}$ = adsorption equilibrium constant for buffering species
$K_{AB,ads}$ = ion-exchange equilibrium constant for a pair of buffering species
K_A = liquid-phase dissociation constant for buffering species, mol/m^3
K_W = dissociation constant for water, mol^2/m^6
N_A = total number of buffering species
q_A = concentration per unit volume of particle, mol/m^3
q_R = total exchange capacity per unit volume of particle, mol/m^3
R_i = ion-exchange functional group in adsorbent
t = time, s
v_{fluid} = interstitial velocity of liquid, m/s
$v_{\Delta C}$ = velocity of a concentration change, m/s
x = axial distance in column, m
z = ionic charge
α = interstitial porosity
ϵ = internal porosity of particle

Superscripts

$+$ = positive charge
$-$ = negative charge
o = uncharged

Subscripts

ads = adsorbed phase
A_i = acidic buffering species
B_i = basic buffering species
d = downstream composition plateau
i = liquid phase
i = component i
I = inert ion
u = upstream composition plateau

Literature Cited

Amersham Pharmacia Biotech Publications, *Chromatofocusing with Polybuffer and PBE*, Uppsala, Sweden (1980).
Bellot, J. C., R. V. Tarantino, and J.-S. Condoret, "Thermodynamic Modeling of Multicomponent Ion-Exchange Equilibria of Amino Acids," *AIChE J.*, **45**(6), 1329 (1999).
Diamond, R. M., and D. C. Whitney, "Resin Selectivity in Dilute to Concentrated Aqueous Solutions," *Ion Exchange: A Series of Advances*, J. A. Marinski, ed., Vol 1, Chapter 8, p. 277, (1966).
Feitelson, J., "Interactions between Organic Ions and Ion-Exchange Resins," *Ion Exchange: A Series of Advances*, J. A. Marinski, ed., Vol 2, Chapter 4, p. 135 (1969).
Frey, D. D., "The Entropy Condition for the Dyamics of Multicomponent Sorption in Porous Media," Chem. Eng. Sci., **45**, 131 (1990).
Frey, D. D., "Mechanism for Glutamic Acid Adsorption on a Weak-Base Ion Exchanger," *Chem. Eng. Sci.*, **52**, 1227 (1997).
Frey, D. D., "Local-Equilibrium Behavior of Retained pH and Ionic Strength Gradients in Preparative Chromatography," *Biotechnol. Prog.*, **12**, 65 (1996).
Frey, D. D., A. Barnes, and J. Strong, "Numerical Studies of Multicomponent Chromatography Employing pH Gradients," *AIChE J.*, **41**, 1171 (1995).
Garcia, A., and C. J. King, "The Use of Basic Polymer Sorbents for the Recovery of Acetic Acid form Dilute Aqueous Solution," *Ind. Eng. Chem. Res.*, **28**, 204 (1989).
Gerberding, S. J. and C. H. Byers, "Preparative Ion-Exchange Chromatography of Proteins from Dairy Whey," *J. Chromatog. A*, **808**, 141 (1998).
Hearn, M. T. W., and D. Lyttle, "Buffer-Focusing Chromatography Using Multicomponent Electrolyte Elution Systems," *J. Chromatog.*, **218**, 483 (1981).
Helfferich, F. G., and B. Bennett, "Weak Electrolytes, Polybasic Acids, and Buffers in Anion Exchange Columns. I. Sodium Acetate and Sodium Carbonate," *Reactive Poly., Ion Exch., Sorbents*, **3**, 51 (1984a).
Helfferich, F. G., and B. Bennett, "Weak Electrolytes, Polybasic Acids, and Buffers in Anion Exchange Columns. II. Sodium Acetate Chloride," *Solvent Extraction Ion Exch.*, **2**, 1151 (1984b).
Helfferich, F. G., and G. Klein, *Multicomponent Chromatography. Theory of Interference*, Marcel Dekker, New York (1970).
Hutchens, T. W., C. M. Li, and P. K. Besch, "Performance Evaluation of a Focusing Buffer Developed for Chromatofocusing on High-Performance Anion-Exchange Columns," *J. Chromatog.*, **359**, 169 (1986a).
Hutchens, T. W., C. M. Li, and P. K. Besch, "Development of Focusing Buffer Systems for Generation of Wide-Range pH Gradients During High-Performance Chromatofocusing," *J. Chromatog.*, **359**, 157 (1986b).
Jansen, M.L., A. J. J. Straathof, L. A. M. van der Wielen, K. Ch. A. M. Luyben, and W. J. J. van den Tweel, "Rigorous Model for Ion Exchange Equilibria of Strong and Weak Electrolytes," *AIChE J.*, **42**, 1911 (1996).
Jones, I., and G. Carta, "Ion Exchange of Amino Acids and Dipeptides on Cation Resins with Varying Degrees of Cross-Linking. I. Equilibrium," *Ind. Eng. Chem. Res.*, **32**, 107 (1993).
Klein, G., J. Sinkovic, and T. Vermuelen, "Weak Electrolyte Ion Exchange in Advanced Technology Water-Reuse Systems," Report No. OWRT/RU-82/7, U.S. Dept. of Interior, Office of Water Research Technology (1982).
Narahari, C., L. Randers-Eichorn, J. C. Strong, N. Ramasubramanyan, G. Rao, and D. D. Frey, "Purification of Green Fluorescent Protein Using Chromatofocusing with a pH Gradient Composed of Multiple Stepwise Fronts" *Biotechnol. Prog.*, **17**, 150 (2001).

Narahari, C., J. C. Strong, and D. D. Frey, "Displacement Chromatography of Proteins Using a Self Sharpening pH Front Formed by Adsorbed Buffering Species as the Displacer," *J. Chromatog. A*, **825**, 115 (1998).

Reichenberg, D., and W. F. Wall, "The Absorption of Uncharged Molecules by Ion Exchange Resins," *J. Chem. Soc.*, **3364** (1956).

Sluyterman, L. A. AE., and O. Elgersma, "Chromatofocusing: Isoelectric Focusing on Ion-Exchange Columns, I. General Principles," *J. Chromatog.*, **150**, 17 (1978).

Sluyterman, L. A. AE., and J. Wijdeness, "Chromatofocusing: Isoelectric Focusing on Ion-Exchange Columns, II. Experimental Verification," *J. Chromatog.*, **150**, 31 (1978).

Strong, J. C. Preparative Protein Purification Using Novel Chromatofocusing Methods PhD Diss., Univ. of Maryland Baltimore County (1997).

Strong, J. C., and D. D. Frey, "Experimental and Numerical Studies of the Chromatofocusing of Dilute Proteins Using Retained pH Gradients Formed on a Strong-Base Anion-Exchange Column," J. Chromatog. A, 769, 129 (1997).

Wankat, P. C., *Rate-Controlled Separations*, Elsevier Applied Science, New York (1990).

Yoshida, H., N. Kishimoto, and T. Kataoka, "Adsorption of Glutamic Acid on Polyaminated Highly Porous Chitosan: Equilibria," *Ind. Eng. Chem. Res.*, **34**, 347 (1995).

Manuscript received Dec. 15, 2000, and revision received Aug. 30, 2001.